Extended U-net for retinal vessel segmentation

Henda Boudegga[1,3[0000-0003-1795-7565]], Yaroub Elloumi[1,3[0000-0001-8878-7562]], Rostom Kachouri[2[0000-0002-9451-4269]], Asma Ben Abdallah[1[0000-0001-7821-7734]], Mohamed Hedi Bedoui[1[0000-0003-4846-1722]]

[1]Medical Technology and Image Processing Laboratory, Faculty of medicine, University of Monastir, Tunisia.
[2]LIGM, Univ Gustave Eiffel, CNRS, ESIEE Paris, F-77454 Marne-la-Vallée France
[3]ISITCom Hammam-Sousse, University of Sousse, Tunisia.

Abstract. The retinal vascular tree is an important biomarker for the diagnosis of ocular dis- ease, where an efficient segmentation is highly required. Recently, various standard Convolutional Neural Networks CNN dedicated for segmentation are applied for retinal vessel segmentation. In fact, retinal blood vessels are presented in different retinal image resolutions with a complicated morphology. Thus, it is difficult for the standard configuration of CNN to guarantee an optimal feature extraction and efficient segmentation whatever the image resolution is. In this paper, new retinal vessel segmentation approach based on deep learning architecture is propounded. The idea consists of enlarging the kernel size of convolution layer in order to cover the vessel pixels as well as moreneighbors for extracting features. Within this objective, our main contribution consists of identifying the kernel size in correlation with retinal image resolution through an experimental approach. Then, a novel U-net extension is proposed by using convolution layer with the identified kernel size. The suggested method is evaluated on two public databases DRIVE and HRF having different resolutions, where higher segmentation performances are achieved respectively with 5*5 and 7*7 convolution kernel sizes. The average accuracy and sensitivity values for DRIVE and HRF databases are respectively in the order of to 0.9785, 0.8474 and 0.964 and 0.803 which outperform the segmentation performance for the standard U-net.

Keywords: Retinal vessel, Segmentation, Convolution kernel size

1 Introduction

The main anatomical components of the retina are the optic disc (OD), the macula and the blood vessels. Retinal blood vessels are represented in the retinal texture with various anatomical criteria, distinguished by the elongated structure, the variety of thicknesses and the curvilinear or the tortuous form.

Several ocular pathologies are associated with abnormal variation of vessel anatomies. As in the proliferative stage of diabetic retinopathy [1], new tortuous vessels appear with lower thickness with respect to the predecessor ones. Further, in the non-proliferative diabetic retinopathy stages, numerous lesions such as microaneurysms

and exudates appear close to the vessel tree [2, 3]. Therefore, the analysis of vascular anatomy is the primary mission to diagnose and detect the ocular pathology severity. Hence, it is indispensable to segment the entire retinal vascular tree.

However, due to the complicated vascular morphologies, their manual segmentation is a tedious task and considered as a challenging step. Therefore, an automatic and an accurate vessel segmentation is required. With the development of deep learning and especially Convolutional Neural Networks (CNNs), various architecture are proposed and have been applied in various medical domains [1, 4, 5]. Certain of these architectures have been propounded for the segmentation tasks such as [6]. However, due to the complicated vessel structures, the standard CNN architectures still insufficient to extract complexes features and guarantee an efficient segmentation whatever the image resolution is and to tolerate the segmentation challenge.

In this work, we propound to put forward a deep learning based method for the segmentation of blood vessels. The idea consists of enlarging kernel size of convolution layer in order to cover the vessel pixels as well as more neighbors for extracting features. Within this objective, the main contribution consists of identifying the kernel size in correlation with retinal image resolution through an experimental approach. Within this context, a novel U-net extension is propounded throw applying convolution layers parameterized by the identified kernel size. The proposed architecture is trained and tested into retinal sub-image datasets, where the produced segmented patches will be merged to generate the final vessel segmentation map. The remainder of this paper is organized into five sections. In section 2, we review some related works based Deep learning architecture. Thereafter, the patch extraction processing is described in section 3. Section 4, the proposed network is detailed. The experimentation results are presented in section 5, where segmentation performances are evaluated and compared to extended networks based methods. The conclusion is given in the last section.

2   Related works

Blood vessel segmentation in fundus imaging was subject of various reviews such as [7], where different categories of approaches have been studied. In this paper, we suggest briefly reviewing Deep learning based approaches.

Several well-known networks have been applied such as Alexnet [8], VGG[9], U-net[6]. However, these networks still insufficient to achieve the segmentation challenge. Within this context, various well- known networks have been extended in order to enhance the segmentation results, as the case of U-net architecture. Certain extension consists of applying advanced convolution layers, as the case of [10, 11] and [12], where standard ones have been replaced respectively by dilated convolution layers and deformable convolution layer. Their aim is respectively to enlarge the convolution receptive field for learning more distributed information and to adapting the convolution receptive field form to the vessel structure. However, their proposed convolution processing still insufficient to properly extract features, where the same dilation rate is applied for all vessel resolutions. In addition, vessels information are

dropped caused by the spaced convolution kernel samples of the dilated convolution kernel.

In addition, other extension consists of varying the size of kernel convolution layers, such as [13], where the convolution kernel size is hierarchically decreased over the network. The aim is to extract hierarchical vessel information and address vessel scale variation. However, the features extracted from the earlier layers will be used for all the remainder of the network, causing a leakage of vessels information.

In other hand, some works suggest improving the performances by further going in depth of the applied architecture as [14]. In this work, the networks AlexNet, LeNet, VGG and ZF-net are modified by further adding convolution layers at the beginning of the network. Nevertheless, the performances of those methods based extended networks have achieved reduced sensitivity rates in the order of 69% and 79%, which are insufficient to gain the segmentation challenge.

3　Patch extraction

As the retina is characterized by a large number of vessels, then a rejected segmentation of the entire image may be achieved. Therefore, a patch extraction process is suggested in this paper, where the fundus images are sliced into sub-images containing a portion of vessels to be segmented separately. The cropping principle allows modeling blood vessels without burdening the patch content. Thus, an experimental study is propounded to determine the appropriate crop size. The experiment consists in iteratively performing several training processes while increasing the cropping size and keeping the training parameters. As a result, experience shows that the 128*128 and 192*192 sizes of patches are the most suitable respectively for DRIVE and HRF images, allowing an appropriate presentation of blood vessels without overloading the crop by several information. This patch extraction process is applied for the process of training and testing. The training patches were extracted from the training images by overlapping with its neighbors to take benefit in increasing the size of the training dataset. In contrast, the testing patches were extracted from testing images without the overlapping strategy. Thereafter, the predicted result was reconstructed with respect to the image size to produce a segmented retinal blood vessel map.

## 4　Proposed architecture for Retinal Blood Vessel Segmentation

The U-net is a CNN architecture characterized by a U-form to segment biomedical images [6]. It is designed with the U-form having the downsampling and upsamling paths, structured on blocks. Containing essentially convolution layers allowing the model to automatically and adaptively detect features.

4

4.1 Convolution processing

The convolution layers of U-net blocks are parameterized by a convolution kernel having the size of "nxn=3x3", applied to extract vessel features to generate a segmentation vessels tree map. The convolution processing is a linear operation, consists of an element-wise multiplication between the weight values "W" of the convolution kernel "K" and the kernel-sized patch of the input feature map "I". Then, the results are summed to obtain an output value in the corresponding position (i,j) of the output feature map "O". This processing is computed as (1), where (Kpx, Kpy) denotes the coordinates of the kernel points.

$$O(i, j) = \sum_{p=0}^{nxn} W(Kp_x, Kp_y) * I(i + Kp_x, j + Kp_y) \tag{1}$$

Upon the extraction of the vessel features, the convolution operation with "nxn=3x3" receptive field is applied to the centered element boxed in red as well as to its local neighbors highlighted in blue in the upper part of Fig.1, iteratively by moving the convolution kernel on the input feature map "I", respecting the same stride on the width and on the length. Nevertheless, as the blood vessels are presented in the retina with a straight structure, characterized by thickness variation and curvilinear or tortuous form, the convolution kernel with tight neighbors as highlighted with blue box in the upper part of Fig.1 cannot cover pixels of the same segment of the image sharing common vessel features. Accordingly, the application of small convolution kernels leads to low feature quality. Consequently, this results in a weak segmentation quality, where the continuity of vessels and their neighbors may not be modeled and detected. In addition, it may be difficult for the small kernels receptive field to distinguish pathological regions, leading to an incorrect segmentation of blood vessels.
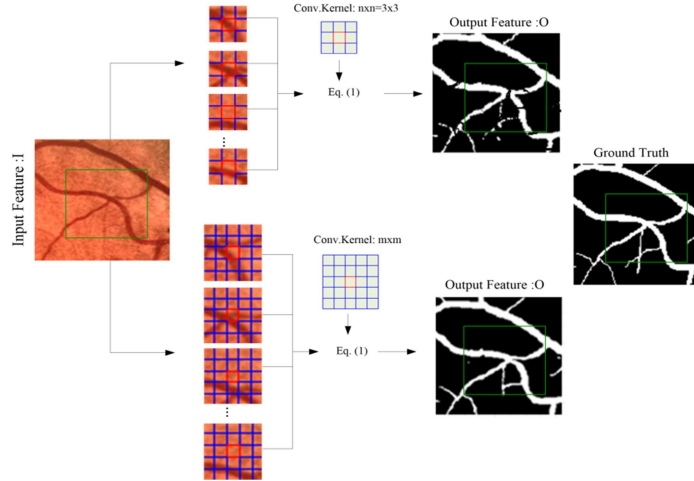
Fig. 1. Segmentation of blood vessels: (Upper part) convolution processing with small convolution kernel size =3x3, (Lower part) Convolution processing with a larger convolution kernel receptive field "mxm".

Within the context of improving the quality of vessels features extraction, the main purpose is to identify the ideal convolution kernel size, which allows extracting optimal vessel features from the earlier layers to be used in the innermost layers.

Thus, the idea is to make the kernel look at more surrounding neighbors while computing the convolution processing as boxed in Fig.1 with blue, in order to compute relevant neighbors and to share more vessel features. Thereupon, the suggestion consists of enlarging the convolution kernel receptive field to "mxm", where "m>3" as shown in the lower part of Fig.1

Therefore, to consolidate the choice of the enlarged convolution kernel size "mxm", an identification approach of the convolution kernel size is proposed and the outline processing is illustrated in Fig.2. The approach consists of continually updating the size of convolution kernel until achieving the suitable convolution kernel size. Hence, the convolution kernel size "mxm is firstly initialized" to "1x1" and the maximal result "Seg_Acc_max" is set to zero. Thereafter, the size of the convolution kernel "mxm" is increased with step equal to two, and the U-net architecture is configured by the increased convolution kernel size. Subsequently, the configured U-net architec- ture is evaluated, where the increased convolution kernel size is saved, if their seg- mentation results "Seg_Acc" is higher than the maximal result "Seg_Acc_max". These treatments are repeated iteratively until obtaining the appropriate kernel size. This identification approach is experimentally described in detail in section 5.2, where two different dataset described in section 5.1 is applied.
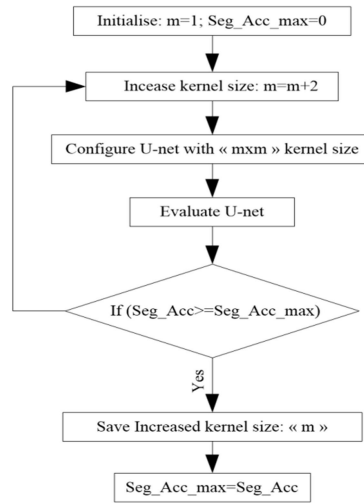

Fig. 2. Flowchart of convolution kernel size identification approach.

4.2 Proposed Network

The main contribution of this work consists in extending the well-known architecture U-net through configuring their convolution layers by a larger convolution kernel having the size of "mxm". The objective is to guarantee accurate performance by

adopting the U-form and making the model able to cover the vessel structure by applying the "mxm" convolution kernel size. As U-net is structured in blocks containing convolution layers having with the same kernel sizes, hence the convolution kernel substitution is applied over the downsample and upsample blocks.

The downsampling path of the extended U-net network is composed by five blocks. Each block is composed of two convolution layers as shown with pink boxes in Fig.3, parameterized by "mxm" convolution kernel illustrated with blue points framed with red as shown in Fig.3. Those convolution layers are configured by a stride "s=1" and activated with the RELU function, in order to avoid the non-linearity of convolution operation. This ReLu is defined as (2), allows setting to zero the negative value "z" of the neuron "x":

$$Relu(x) = Max(0, z) \tag{2}$$

Each block of the downsampling path excepting the last is composed of two convolution layers followed by a max pooling layer as illustrated with red arrows in Fig.3. This layer is parameterized by a pooling window having the size "pxp=2x2" and a stride "s=2", allows taking the maximum value of the pooling window of the input feature map "I". Hence, the size of the output feature map is defined in (3). For the first downsampling block, 64 feature maps are convolved. Thereafter, the number of output feature maps is doubled as shown in Fig.3.

$$Out\_Maxpool = Floor(I - p/s) + 1 \tag{3}$$

Similarly to the original U-net architecture, the upsampling path is mirrored to dowsampling path, where four blocks are deployed. Each of which is composed by upsampling layer as illustrated with green arrows in Fig.3, followed by two convolution layers having the same configuration as downsampling convolution layers. The applied upsampling layers are parameterized by a kernel size "nxn=2 × 2" and a stride "s=2", allows reproducing the spatial size and information of the image. Thus, the output feature map size can be calculated as (4), where "M" corresponds to the input image size and the padding is set to zero.

$$Out\_Up = (M - 1) * 2 + n - 2 * padding \tag{4}$$

Contrary to the downsampling path, the number of the output feature map is reduced by half for each block, as shown in Fig.3. The network is achieved by a 1x1 convolution layer activated with the softmax function as shown with a purple box in Fig.3, allows the mapping of 64 feature maps to produce the prediction of vessels and background. Furthermore, a skip connection between the downsampling blocks and their corresponding of the upsampling blocks illustrated with grey arrows is per- formed, promoting the fusion of the lower details information with the global information.
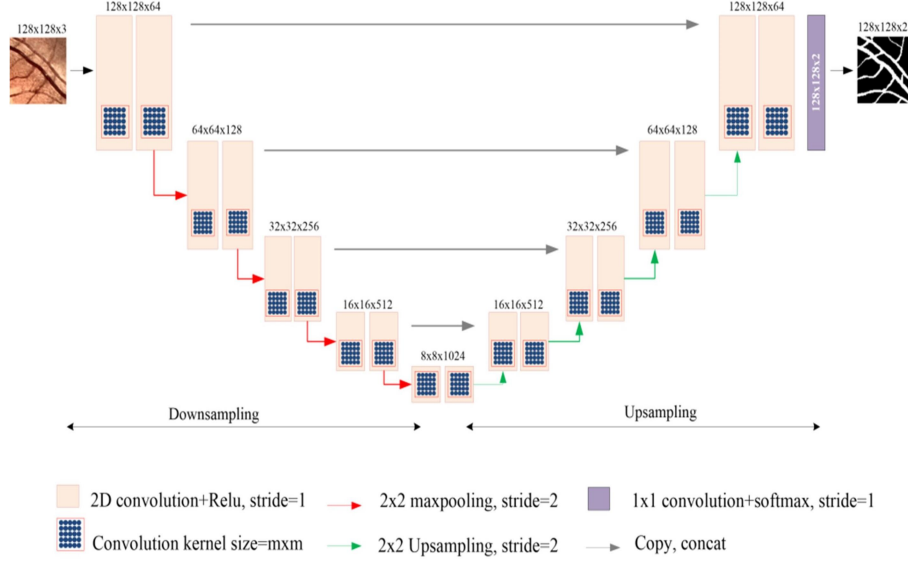
Fig. 3. Proposed network for retinal blood vessel segmentation method

4.3 Training Parameter Setting

The suggested network is conducted for a training process, to modify the node weights until having an accurate model. This processing is performed using a set of training parameters, where several ones are chosen experimentally, while others are used by referring to recent studies. As for the optimizer and the learning rate value, some training experiences are conducted while modifying for each experience the value of one parameter. Thereafter, we select the one performing the higher result rates. Hence, the ADAM optimizer parameterized with learning equal to 0.001 is chosen for training the proposed network. Furthermore, the Xavier initialization technique is applied. Added to that, to minimize the gap between the predicted output and the ground truth, the cross entropy "CE" loss function defined in (5) is applied, where "P_out" and "d_out" respectively correspond to the predicted output and the desired one.

$$CE = -\sum(d_{out}.\log(P_{out}) + (1 - d_{out}).\log(1 - P_{out})) \tag{5}$$

In the same vein, the dropout regularization technique is applied for regularizing the training, which consists in temporarily switching a subset of nodes. The applied technique is defined in (6), where "L_Out" corresponds to the layer output, "F" is the activation function of the weight matrix "W" of layer "x", and "1-d_p" is the dropout mask where the "d_p" value is chosen experimentally and is set to 0.5.

$$L\_Out = F(W_x)(1 - d_p) \tag{6}$$

5 Experiments

The method is evaluated with respect to its background through using well-known retinal image database and computing the evaluation metrics described in sub-section 5.1. The experiment is carried out by distinctly identifying the convolution kernel size and evaluating the segmentation performance respectively in sub-section 5.2 and 5.3. Further a comparative assessment with respect to the state-of-the-art methods detailed in sub-section 5.4.

5.1 Dataset, Evaluation metrics and Experiment setup

Dataset: The validation of the proposed method is ensured by the deployment of the public retinal database DRIVE [7] and HRF [7]. Both databases are composed respectively by 40 and 45 retinal images with different resolution   respectively in the order of 565 × 584 and 3504x2336. Those retinal images are joined with its manual blood vessel segmentation and its masks. For the DRIVE database, seven retinal images are characterized by the signs of diabetic retinopathy [7]. In Addition, 30 HRF retinal images have the signs of proliferative diabetic retinopathy and glaucoma [7].

Evaluation metric: Four classes of pixel classification results, namely True Positive (TP), True Negative (TN), False Positive (FP) and False Negative (FN), can be generated depending on the correct or incorrect segmentation of pixels, with respect to the manual annotation of blood vessel segmentation. Various evaluation metrics can be conducted from these pixel classification results, including Accuracy (Acc), sensibility (Sens), specificity (Spec) and DICE, where Sensitivity is the indicator that reflects the proportion of positives correctly identified. All those evaluation metrics are computed respectively as in (7-10).

$$Accuracy(Acc) = TN + TP/(TP + FP + FN + TN) \tag{7}$$

$$Sensitivity(Sens) = TP/(TP + FN) \tag{8}$$

$$Specificity(Spec) = TN/(TN + FP) \tag{9}$$

$$DICE = 2 * TP/((2 * TP) + FN + FP) \tag{10}$$

Experiments setup: All the experiments are done on Intel core i7 configured with a 3.67 GHZ frequency processor, 8Go RAM and a NVIDIA GTX 980 GPU. This method is implemented with the Python 3.5.2, the OpenCV library 3.4 and Tensorflow GPU framework 1.12, using CUDA 9.0 with CUDNN 7.6.3.

5.2 Identification of Convolution Kernel Size

We suggest in this section, implementing the identification approach of the convolution kernel size proposed in section 4.2. Within this context, we suggest iterating three times throw configuring the architecture U-Net respectively with three different kernel sizes in the order of 3x3, 5x5 and 7x7. The aim is to identify the suitable con-

volution kernel sizes correlated with vessel representation into DRIVE and HRF images patches. For this experiment, both DRIVE and HRF are processed where three segmentation measurements are depicted in Table 1 for the different U-Net configuration.

Form Table 1, the three different convolution kernel size have depicted Acc and Spec rates respectively greater than 95% and 97% of the two databases . Nevertheless, the miss segmentation of the thin-vessel pixels hardly affects the Acc and Spec rates. On other hand, the Sens rate increases with the correct extraction of fine vessels and maintain of connectivity, where the numbers of false positives pixels are reduced and the true positives pixels are increased. Thus, the higher Sens rates in the order of 86% and 80% generated respectively by the 5x5 U-net kernel size configuration of DRIVE and 7x7 U-net kernel size configuration of HRF. Those Sens rates indicate the ability of models to generate accurate segmentation of retinal vessels. Accordingly, we can confirm that using of these larger kernel sizes for both databases can reduce the number of false positives and increased the true positives. Further, for the case of DRIVE images shown in Fig.4, the largest U-net configuration with 7x7 kernel samples disperses and drops vessel information. In contrast, it is revealed that the U-net configuration with the enlarged convolution kernel size in the order of 5x5 can more accurately detect the retinal vessels, with respect to the other U-net configuration. Moreover, the propounded network preserves more the connectivity of vessel tree with respect to the other configuration.

Table 1. Average performance for the 3 different Convolution kernel sizes of U-net on DRIVE and HRF databases.

Convolution kernel size	DRIVE			HRF		
	Acc	Sens	Spec	Acc	Sens	Spec
3x3(original U_net)	0.9594	0.7698	0.9798	0.9577	0.6577	0.9701
5x5	0.9759	0.86	0.9853	0.958	0.78	0.975
7x7	0.975	0.5916	0.9982	0.964	0.803	0.963

5.3   Segmentation performance

We suggest evaluating the suggested U-net extension for both DRIVE and HRF basing on the Acc, Sens, Spec and DICE metrics. Fig. 5 shows examples of segmentation results. Further, within the aim of evaluating the robustness of the suggested method across the testing images, we suggest applying the four-fold cross validation approach on DRIVE database as proposed in [15]. Hence, the retinal fundus images are splitted into four subsets, three are conducted for the training process and one subset is used for testing. Therefore, four experiments are performed, where the average performance measurements of the four experiments are indicated in Table 2. Consequently, the U-net extension have confirming a higher segmentation performance of the proposed network whatever the image used for the training or testing procedure.
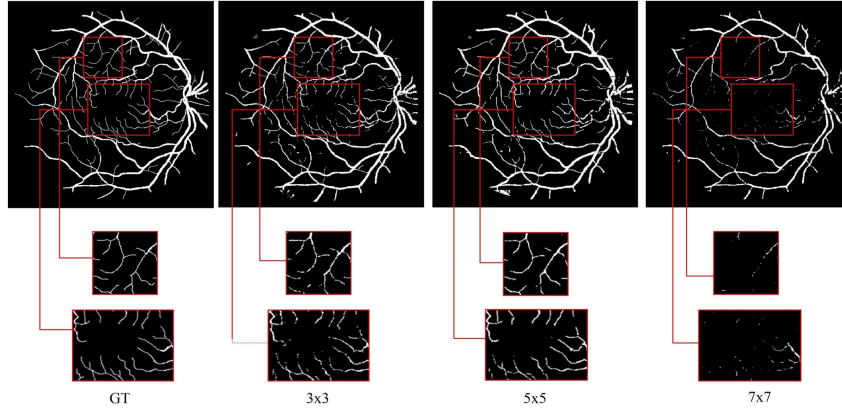
Fig. 4. Comparison of segmentation results of different U-net configuration on DRIVE images; (Row 1) segmentation vessel maps, (Row 2) local thin vessel region of fundus images, (column 1) ground truth, (column 2-4) segmentation result generated respectively by 3x3, 5x5 and 7x7 U-net configuration
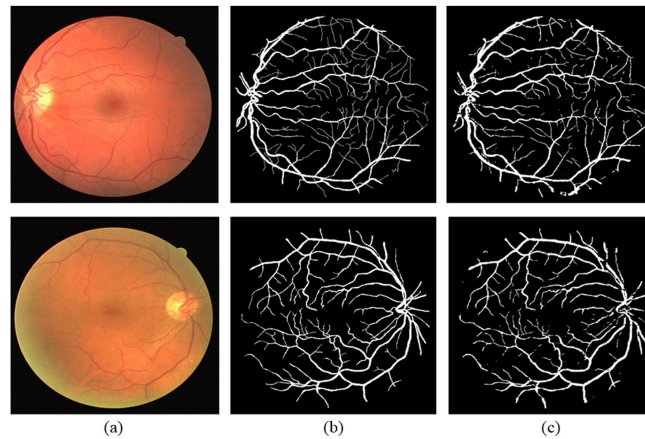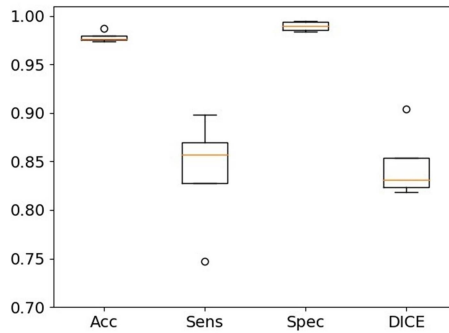

Fig. 5. Segmentation results for DRIVE database; (a) Retinal images, (b) Ground truth, (c) Segmented results.

Table 2. Average performance of DRIVE and HRF database.

Database	Acc	Sens	Spec	DICE
DRIVE	0.9785	0.8474	0.9892	0.8461
HRF	0.964	0.803	0.9637	0.778

To evaluate the robustness of the U-net extension for DRIVE database and confirm a higher correlation with respect to the used images, the box plots in Fig.6 illustrate the four performances Acc, Sens, Spec and DICE measures of the four experiments. The representation demonstrates a high correlation between 4-fold datasets, where the Acc

values are very close to their average with a variation in the order of 0.01. Reduced gaps are also deduced between values for Sens, Spec and DICE with variation values, are respectively in the order of 0.0462, 0.0047 and 0.028 for the DRIVE database.

Fig. 6. Boxplot of four-fold cross validation results.

5.4 Comparison with state of the art

To evaluate the propounded method, we compare our segmentation performance on DRIVE database with the state-of-the-art methods. Thus, we propose to evaluate our segmentation results with respect to standard-DL-based methods and extended-DL-based methods, where the Acc, Sens and Spec values on the DRIVE database are presented in Table 3. From these results, we deduce that the proposed average Sens rate is better than the extended-DL-based methods [10], [11], [13], [12], and [14] and the standard DL based methods [8] and [6], where a significant difference in the range of 0.12 is distinguished. Sensitivity is a particular indicator in the context of segmentation. It shows the capability of the model to detect the discrete details of vessels. Hence, the proposed network presents a powerful ability to detect vessel pixels. This relevant performance is explained by the growth of the receptive field vision of the convolution kernel, where a single pixel in a 5x5 activation map is able to look at every 5x5 region of the input feature map. As a consequence, such increase in the receptive field vision allows modeling vessel neighborhood and learning deeper vessel details similar to ground truth segmentation. In the same vein, the contribution put forward in [10] consists in enlarging the receptive field convolution kernel by applying dilated convolution layers. However, a reduced Sens rate compared to ours is generated in the order of 0.79. Thus, the reduction is explained by the applied dilation rate, which introduces striding between the kernel samples that result in the drop of information and vessel features.

Table 3. Comparison of segmentation performances on DRIVE database

	works	DRIVE		
Standard DL architecture-based methods		Acc	Sens	Spec
	[8]: Alexnet	0.9624	0.754	0.9825
	[6]: U-net	0.9594	0.7698	0.9798
Extended DL architectures based methods	[10]: EEA-U-net	0.9577	0.7918	0.9708
	[11]: D-U-net	0.9641	0.7595	0.98
	[13]: Joint loss U-net	0.9542	0.7653	0.9818
	[12]: MA-U-net	0.9557	0.789	0.9799
	[14]: M-Alexnet	0.9628	0.7995	0.9804
	[14]: M-VGG	0.9585	0.8404	0.9802
Proposed method(average)		0.9785	0.8474	0.9892

6   Conclusion

The segmentation of the retinal vessel tree is an indispensable element for the detection and diagnosis of ocular and cardiovascular diseases. Thus, the clinical contexts expect precise and sensitive segmentation of blood vessels. Within this objective, an identification of convolution kernel size in correlation with vessel representation on different retinal image resolution is propounded. Thus, the convolution kernel size is enlarged in order to cover the vessel pixels as well as more neighbors for extracting features.

On other hand, several automatic ophthalmological diagnostic systems such as [16], [17] and [18] expect sensitive segmentation of retinal vascular tree. In this context, our automated method can be directly employed to take benefit from its segmentation performance. As future work, the method proposed in [18] can be extended in function to this approach in order to take benefit to the accurate segmentation performance while keeping computation time.

References

1. M. Akil, Y. Elloumi, R. Kachouri, "Detection of Retinal Abnormalities in Fundus Image Using CNN Deep Learning Networks", Book Title: State of the Art in Neural Networks, Volume Number: Vol. 1, Publisher: Elsevier, 2020.
2. Kaur, J., & Mittal, D. A generalized method for the segmentation of exudates from pathological retinal fundus images. Biocybern. Biomed. Eng, 38(1), 27-53, (2018).
3. Y. Elloumi, N. Abroug, M. Hedi Bedoui. "End-to-End Mobile System for Diabetic Retinopathy Screening Based on Lightweight Deep Neural Network", The Int. Intell. Data Anal., (2022).
4. Y. Elloumi, Cataract grading method based on deep convolutional neural networks and stacking ensemble learning, Int. J. Imaging Syst. Technol., 798-814, (2022).
5. Y. Elloumi, M.Akil, H.Boudegga, Ocular diseases diagnosis in fundus images using a deep learning: approaches, tools and performance evaluation. Real-Time Image Processing and Deep Learning SPIE, Vol. 10996, pp. 221-228, (2019).

6. O. Ronneberger, P. Fischer, and T. Brox, 'U-Net: Convolutional Networks for Biomedical Image Segmentation', in Med Image Comput Comput Assist Interv (MICCAI), pp. 234–241, (2015).

7. M. M. Fraz et al., 'Blood vessel segmentation methodologies in retinal images – A survey', Comput. Methods Programs Biomed, vol. 108, no. 1, pp. 407–433, (2012).

8. Krizhevsky, I. Sutskever, and G. E. Hinton, 'ImageNet classification with deep convolutional neural networks', Commun. ACM, vol. 60, no. 6, pp. 84–90, (2017).

9. V. Badrinarayanan, A. Kendall, and R. Cipolla, 'SegNet: A Deep Convolutional Encoder-Decoder Architecture for Image Segmentation', arXiv:1511.00561, (2016).

10. S. V. and I. G., 'Encoder Enhanced Atrous (EEA) Unet architecture for Retinal Blood vessel segmentation', Cogn. Syst. Res, vol. 67, pp. 84–95, (2021).

11. Q. Jin, Z. Meng, T. D. Pham, Q. Chen, L. Wei, and R. Su, 'DUNet: A deformable network for retinal vessel segmentation', Knowl.-Based Syst., vol. 178, pp. 149–162, (2019).

12. H. Li et al., 'MAU-Net: A Retinal Vessels Segmentation Method', in 2020 42nd Annu. Int. Conf. IEEE Eng. Med. Biol Society (EMBC), pp. 1958–196, (2020).

13. Z. Yan, X. Yang, and K.-T. Cheng, 'Joint Segment-Level and Pixel-Wise Losses for Deep Learning Based Retinal Vessel Segmentation', IEEE Trans. Biomed. Eng., vol. 65, no. 9, pp. 1912–1923, (2018).

14. Q. Jin, Q. Chen, Z. Meng, B. Wang, and R. Su, 'Construction of Retinal Vessel Segmentation Models Based on Convolutional Neural Network', Neural Process. Lett., vol. 52, no. 2, pp. 1005–1022, (2020).

15. H. Boudegga, Y. Elloumi, M. Akil, M. Hedi Bedoui, R. Kachouri, and A. B. Abdallah, 'Fast and efficient retinal blood vessel segmentation method based on deep learning network', Comput. Med. Imaging Graph., vol. 90, p. 101902, (2021).

16. R. Boukadida, Y. Elloumi, M. Akil, M. Hedi Bedoui, 'Mobile-aided screening system for proliferative diabetic retinopathy'. Int. J. Imaging Syst. Technol, (2021).

17. Y. Mrad, Y. Elloumi, M. Akil, M. Hedi Bedoui, 'A Fast and Accurate Method for Glaucoma Screening from Smartphone-Captured Fundus Images', IRBM (2021).

18. S. B.Sayadia, Y. Elloumi, M. Akil, M. Hedi Bedoui, R. Kachouri, and A. B. Abdallah, "Automated Method for Real-Time AMD Screening of Fundus Images Dedicated for Mobile Devices", Med Biol Eng Comput, 60, 1449–1479 (2022).